Signal-to-noise ratio gain of a noisy neuron that transmits subthreshold periodic spike trains

Yan Mei Kang,[1,2,*] Jian Xue Xu,[2] and Yong Xie[2]
[1]*Institute of Information and System Science, School of Science, Xi'an Jiaotong University, Xi'an 710049, China*
[2]*Institute of Nonlinear Dynamics, School of Architectural Engineering and Mechanics, Xi'an Jiaotong Universtiy, Xi'an 710049, China*
(Received 3 November 2004; published 2 August 2005)

The transmission properties of an integrate-and-fire neuron model that transmits coherent subthreshold spike trains in a shot noise environment are investigated by numerical simulation. For very weak coherent couplings, it is shown that the input-output signal-to-noise ratio (SNR) gain is easier to exceed unity; while for stronger coherent couplings it is difficult to observe the SNR gain larger than unity at the optimal noise intensity. These observations are different from those acquired in the case of continuous noise. Our analysis further suggests that the larger SNR gain in the very weak coherent coupling case should be due to the noise-induced resonance. It is also shown that there is more possibility of the SNR gain above unity for slower periodic spike trains transmitted by the model. The results may be useful in understanding the performance of real noisy neurons acting as signal-processing elements.

DOI: 10.1103/PhysRevE.72.021902 PACS number(s): 87.10.+e, 02.50.−r, 05.40.−a

I. INTRODUCTION

The phenomenon of stochastic resonance (SR) was initially proposed in the context of the explanation of the climatic periodicity, wherein an optimal amount of noise makes the Kramers rate of a bistable system coincide with the drive frequency, and as a result the output signal-to-noise ratio (SNR) attains the maximum [1,2]. During the past 20 years, the phenomenon has attracted intensive attention beyond bistable systems, such as the evidences of it have been well documented in underdamped systems [3,4], excitable systems [5,6], threshold devices [7,8], etc., here to name but a few. Since neurons in the brain engage in complex and very efficient signal-processing operations in noisy environments, plenty of neurophysiological experimental prototypes have dedicated to investigate the effects of noise on neurons (see Ref. [2] for a review). Up to now the possibility that noise helps neurons in the detection and transmission of subthreshold signals by means of SR has been proved extensively, which greatly changes the old opinion that noise decreases the responsiveness of neurons, but whether neurons indeed use it still deserves confirmations. This motivates further investigations both into the experiments and the excitable models to explore the conditions under which SR occurs. Among these investigations, whether the output SNR can exceed the input SNR, or whether the output signal can be less noisy than input signal at the optimal noise intensity of SR is another interesting question. The problem is often referred to as the SNR gain [7–14].

The SNR gain has been demonstrated in systems including the level crossing detector [7], the static resonator [8], the Schmitt trigger [10–12], the double well potential [13], the Hodgkin-Huxley neuron model [14], etc. Since the proof that there is no SNR gain in the small coherent signal limit with Gaussian white noise (i.e., within the linear response theory) has been given [9,15], most of the research was confined to the case of the coherent pulselike signals or to the case with other types of noise so that the linear response theory was circumvented. The stochastic excitation considered in all these cases is continuous noise, however, and there is no report of the SNR gain in the case of short noises. Since spike trains are the most basic forms by which most neurons communicate with each other, and recent neuralphysiological studies [16–19] on their stochastic nature suggested that a Poisson process can mimic the disturbance in interspike intervals (ISIs), using the shot Poisson noise to model the background spike activities in the synaptic input is quite natural. Therefore, in this paper we demonstrate the SNR gain in this case by using an integrate-and-fire neuron model with synaptic inputs involved a coherent component and a random component, both modeled by discrete pulse trains, and we expect to have an understanding of the case.

In the next section, the critical amplitude of the neuron model and the numerical method we adopt are expounded. In Sec. III, the detailed numerical results of the SNR gain are given and analyzed. In Sec. IV, discussions and conclusions are presented.

II. MODEL AND METHOD DESCRIPTION

We consider the classical integrate-and-fire neuron model [18]. Under the threshold V_{th}, the neuron membrane, of time constant τ_m, has its electric potential $V(t)$ controlled by

$$\tau_m \frac{dV}{dt} = -V + w_s s(t) + w_\eta \eta(t). \tag{1}$$

As input signals on $V(t)$, the coherent component $s(t) = \Sigma_n \delta(t - nT_s)$ is a periodic spike train with period T_s, which carries the information of cognitive processes, while the noise component $\eta(t) = \Sigma_n \delta(t - t_k)$ with t_k's to be the random spike instants resulting from the background spike activities is described by homogenous Poisson-distributed random pulses of density $1/T_\eta$ and the autocorrelation function $R_{\eta\eta}(\tau) = \langle \eta(t)\eta(t+\tau)\rangle = (1/T_\eta)\delta(\tau) + (1/T_\eta)^2$. For the sake of

*Electronic address: kangyanmei2002@yahoo.com.cn

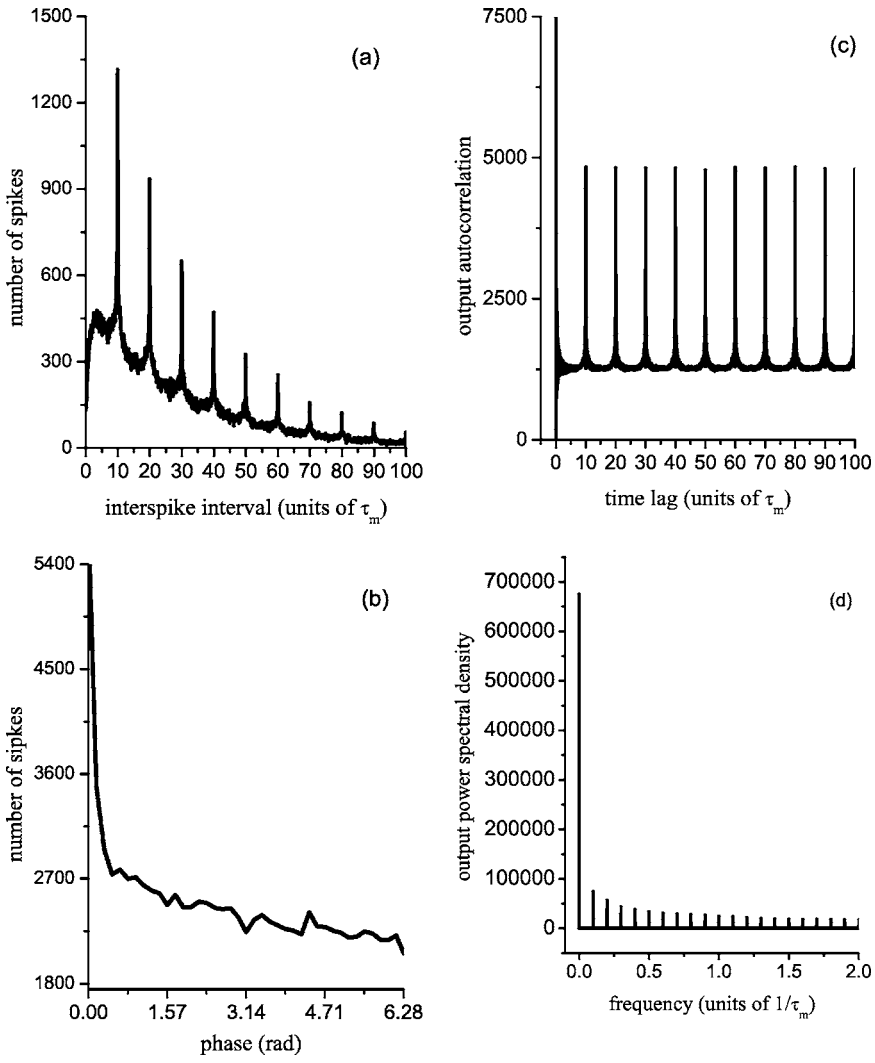

FIG. 1. An example of calculated (a) interspike interval histogram, (b) periodic histogram, (c) autocorrelation function, and (d) power spectral density of an output spike train. $T_\eta=0.125\tau_m$, $w_s=w_\eta=0.5\hat{w}_s$.

convenience, T_η will be refereed to as the noise intensity parameter in the following. The parameters w_s and w_η are synaptic couplings for the coherent input and the noise pathways, respectively. Once the membrane potential $V(t)$ reaches the threshold V_{th} , a spike is discharged by the neuron, and then the membrane potential is immediately reset to zero, from where $V(t)$ evolves again according to Eq. (1). The output of the neuron is usually recorded as $y(t)=\Sigma_n\delta(t-t_n)$, where t_n is the nth instant when the neuron is discharging. Let us temporarily assume there is no noise in Eq. (1), namely $w_\eta=0$ then Eq. (1) turns into

$$\tau_m\frac{dV}{dt}=-V+w_s\sum_n\delta(t-nT_s). \tag{2}$$

It is clear that the solution of Eq. (2) reads

$$V(t)=\frac{w_s}{\tau_m}\sum_{n=0}^{\infty}\exp\left(-\frac{1}{\tau_m}(t-nT_s)\right)H(t-nT_s), \tag{3}$$

where $H(.)$ is the unit step function defined as

$$H(t)=\begin{cases}1, & t\geqslant 0\\ 0, & t<0.\end{cases}$$

Supposing $t\geqslant NT_s$, one defines

$$S_N(t)=\frac{w_s}{\tau_m}\sum_{n=0}^{N}\exp\left(-\frac{1}{\tau_m}(t-nT_s)\right)H(t-nT_s), \tag{4}$$

then

$$\begin{aligned}S_N(t)&=\frac{w_s}{\tau_m}\left[\exp\left(-\frac{t}{\tau_m}\right)+\exp\left(-\frac{t-T_s}{\tau_m}\right)+\cdots\right.\\&\quad\left.+\exp\left(-\frac{t-NT_s}{\tau_m}\right)\right]\\&\leqslant\frac{w_s}{\tau_m}\left[\exp\left(-\frac{NT_s}{\tau_m}\right)+\exp\left(-\frac{(N-1)T_s}{\tau_m}\right)+\cdots+1\right]\\&=\frac{w_s}{\tau_m}\frac{1-\exp(-NT_s/\tau_m)}{1-\exp(-T_s/\tau_m)}\\&=\max(S_N(t)).\end{aligned} \tag{5}$$

Let $t\to\infty$ and $N\to\infty$, then

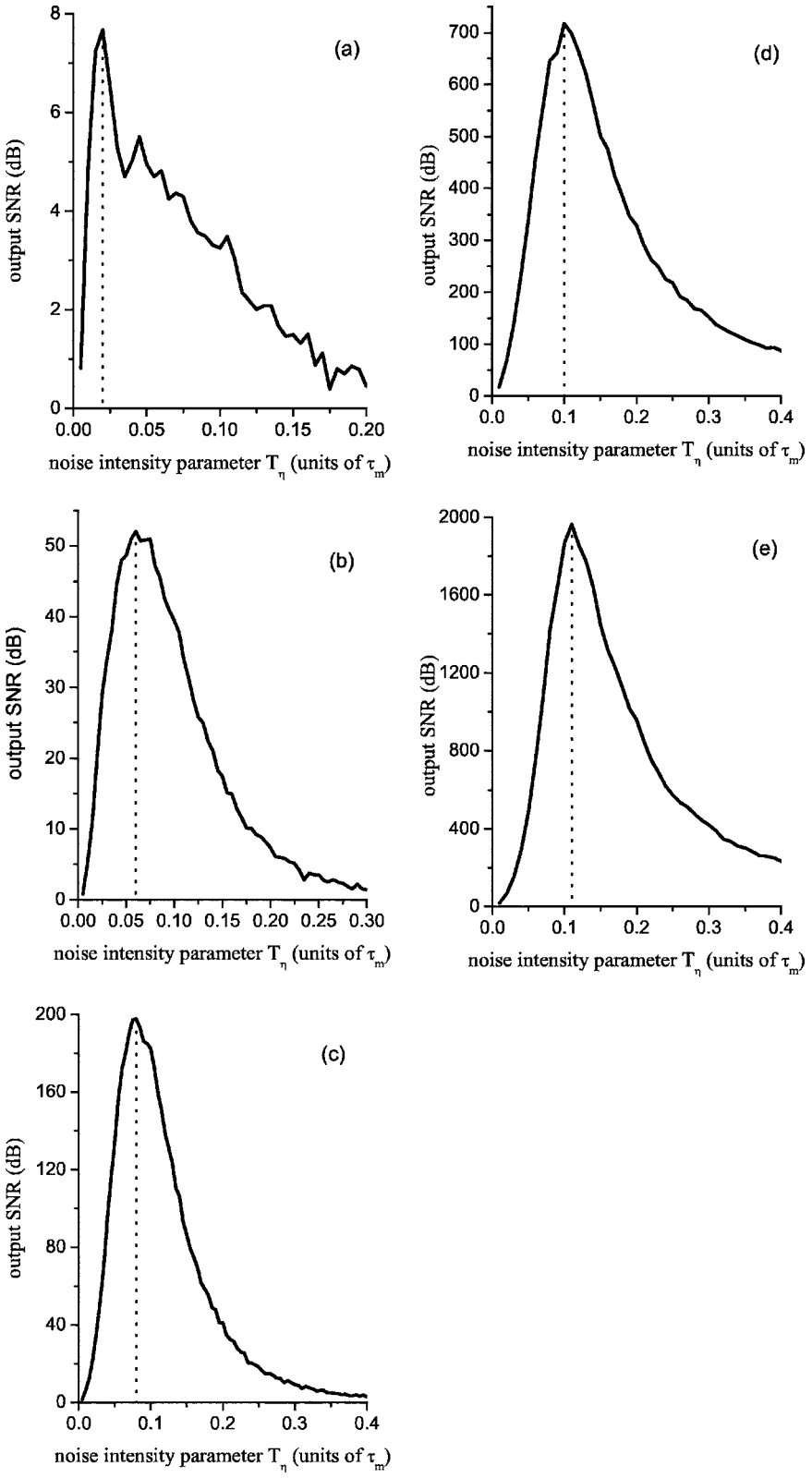

FIG. 2. Dependence of the output SNR on noise intensity parameter T_η for different coherent couplings where the vertical dot lines denote the optimal noise intensity parameters. $w_\eta = 0.5\hat{w}_s$, $T_s = 10\tau_m$, w_s is (a) 0.1, (b) 0.3, (c) 0.5, (d) 0.7, and (e) 0.9 $\hat{w}_s$.

$$V_{\max} = \lim_{N\to\infty} \max(S_N(t)) = \left(\frac{w_s}{\tau_m}\right)\left[1 - \exp\left(-\frac{T_s}{\tau_m}\right)\right]^{-1}. \quad (6)$$

Let $V_{\max} = V_{\text{th}}$, then the critical amplitude of the coherent coupling is

$$\hat{w}_s = \tau_m V_{\text{th}}\left[1 - \exp\left(-\frac{T_s}{\tau_m}\right)\right]. \quad (7)$$

From Eq. (7) we see that if the coherent spike train is subthreshold, i.e., $w_s < \hat{w}_s$, the membrane potential cannot reach

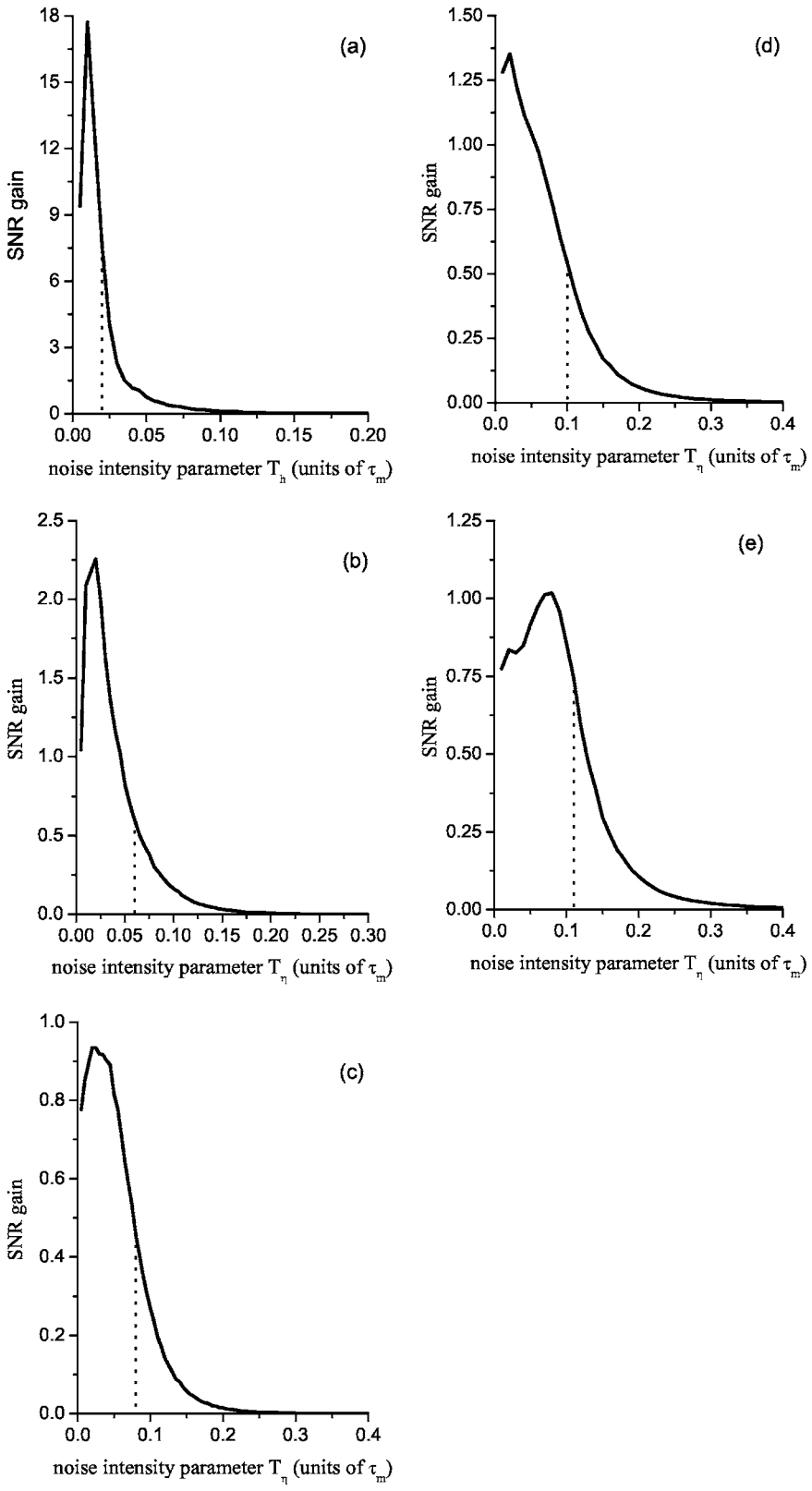

FIG. 3. Dependence of the SNR gain on noise intensity parameter T_η for different coherent couplings. The parameters are the same as those in Fig. 2.

the threshold without noise, so the neuron of model (1) cannot generate discharge, and the subthreshold periodic spike train cannot be transmitted to other neurons. It suggests that noise can assist the central neurons to transmit information by means of SR, as reported in Ref. [18], but whether there is a SNR gain larger than unity at the optimal noise intensity of SR has not been reported before.

Since the existing methods such as Gaussian approximations [20,21] for calculating the probability density of the ISIs of Eq. (1) are only applicable to the case of $w_s=0$, we

investigate the SNR gain by means of numerical simulation. Noting that the intervals between random instants are mutually independent random variables with an identical exponential distribution of parameter $1/T_\eta$, the instants when the driving neurotransmitters or spikes arrive are generated according to $t_k = t_{k-1} - \ln(T_\eta u_k)$ with $t_0 = 0$ and u_k being uniformly distributed random numbers in $[0,1]$ for $k \geqslant 1$. To integrate Eq. (1) for the output spike train, an Euler scheme with time step $\Delta t = 10^{-2}\tau_m$ is used. Suppose $\{t_k\}_{k=0}^{\infty}$ is an output spike train recorded in a time span $[0,T]$ with $T = 5.0 \times 10^4 \tau_m$, then the interspike interval histogram, periodic histogram, autocorrelation, and the output power spectral density can be calculated as the average of 100 such recordings. For instance, for a spike recording, the power spectral density is $P(\omega) = |F(\omega)|^2$, with

$$F(\omega) = \frac{1}{2}\sum_n \exp(n\omega t_n)\left[1 - \cos\left(\frac{2\pi t_n}{T}\right)\right], \tag{8}$$

which is the Fourier transform with Hanning windows of the spike train, and the average of 100 such power spectral densities is taken as the output power spectral density. Figure 1 is a numerical example. The output ISI histogram in Fig. 1(a) is stochastic but tends to be a multipeaked distribution at multiples of the signal period T_s, which shows that the output spike train contains the coherent information. The periodic histogram describes the distribution of the spike numbers over the whole phase interval [22], and the spikes are random but prefer a certain phase near zero in Fig. 1(b). The output spike train in Fig. 1(c) is temporally correlated, especially obvious at the multiples of T_s , while the spectral density of the output spike train in Fig. 1(d) concentrates at the multiples of the coherent frequency $1/T_s$. For a given power spectral density, both the SNR on the input and that on the output of Eq. (1) are defined as

$$R = \frac{P(1/T_s) - N(1/T_s)}{N(1/T_S)}, \tag{9}$$

where $P(1/T_s)$ stands for the spectral density at the coherent frequency, $N(1/T_S)$ signifies the spectral density of the background noise measured by averaging the 40 spectral density amplitudes around but not including $P(1/T_s)$, where the spectral bin is chosen to be $(1/T_S)/100$. And then the SNR gain is defined as

$$G = \frac{R_{\text{out}}}{R_{\text{in}}}, \tag{10}$$

where R_{out} and R_{in} represent the SNRs on input and output, respectively. If at the optimal noise intensity there is $G > 1$, then one says that the input signal can be improved by adding noise through SR. This is just the point concerned in the SNR gain investigation.

III. NUMERICAL SIMULATION OF SR AND SNR GAIN

In the following, we take all coherent input signals to be subthreshold, namely, they satisfy $w_s < \hat{w}_s$. The curves of the output SNR via noise intensity parameter and the curves of the SNR gain via noise intensity parameter are shown in Figs. 2 and 3, respectively. The output SNR curves exhibit typical bell-shaped SR characteristic as reported in Ref. [18]. By comparing Figs. 2 and 3 one sees that for stronger coherent couplings such as $w_s \geqslant 0.5\hat{w}_s$, the SNR gain at the optimal noise intensity parameter marked with a dot line becomes larger as the coherent coupling becomes stronger, but SNR gain does not reach unity in these cases as shown in Figs. 3(c)–3(e). For the weaker coherent couplings, however, the variability in the SNR gain at the optimal noise intensity is toward a contrary direction, and Fig. 3(a) shows that the SNR gain at the optimal noise intensity is larger than unity for the weakest coherent coupling $w_s = 0.1\hat{w}_s$. This observation is different from those obtained in Refs. [7,8], where according to the type of continuous noise, the SNR gain at the optimal noise intensity always increases as the coherent

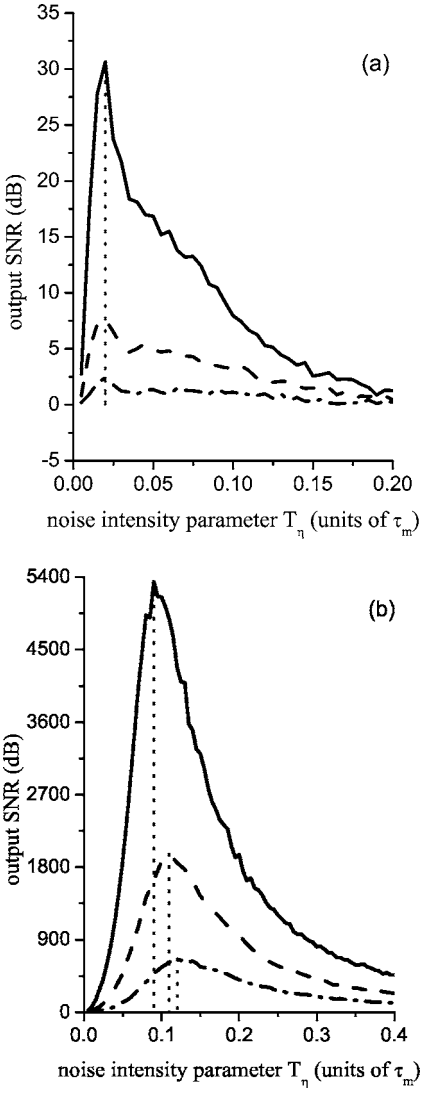

FIG. 4. Dependence of the output SNR on noise intensity parameter T_η. $w_\eta = 0.5\hat{w}_s$ and w_s are (a) 0.1 and (b) 0.9 $\hat{w}_s$, respectively. The solid curve corresponds to $T_s = 5\tau_m$, the dashed curve corresponds to $T_s = 10\tau_m$, and the dash-dotted curve corresponds to $T_s = 20\tau_m$. The vertical dot lines denote the optimal noise intensity parameters.

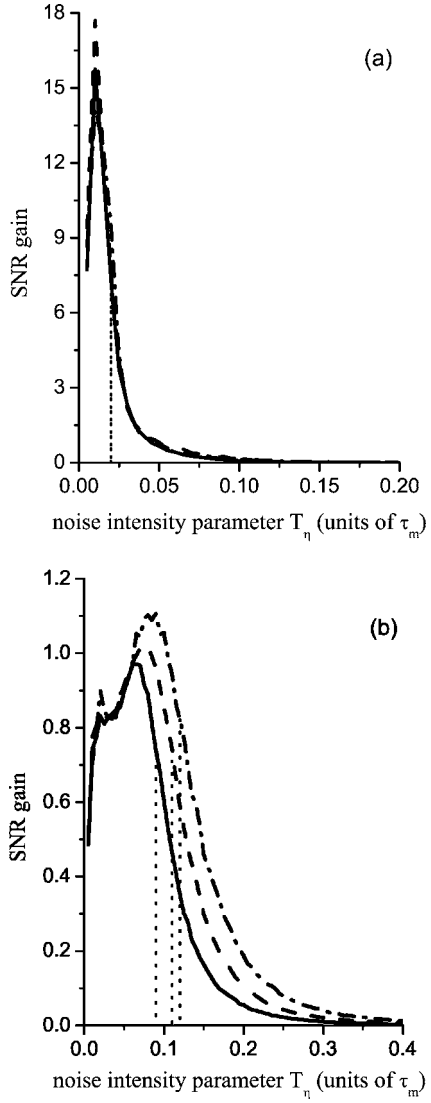

FIG. 5. Dependence of the SNR gain on noise intensity parameter T_η. The parameters are the same as those in Fig. 4.

input amplitude decreases or increases. Moreover, for all periodic pulse trains considered in Refs. [7,8], the output SNR can be improved through SR, but here the output SNR can be improved by SR only when the coherent coupling is quite weak.

To further support the above observation, we also give numerical results for coherent inputs with different periods as shown in Figs. 4 and 5. By comparing these figures, again one sees that for the large coherent coupling $w_s=0.9\hat{w}_s$ as shown in Fig. 5(b), the SNR gain cannot attain unity at the optimal noise intensities, while Fig. 5(a) shows that it exceeds unity at the optimal noise intensities for the weak coherent coupling $w_s=0.1\hat{w}_s$ in all three cases considered. This suggests that the above observation should be the general characteristics of Eq. (1). Here, we emphasize that although the optimal noise intensity parameters in different cases of Fig. 4(a) are the same under our parameter axis scale, the fact that they decreases as the coherent period reduces can be identified at a more refined scale (the figure is omitted). In addition, by checking Fig. 5(b), one observes that the SNR

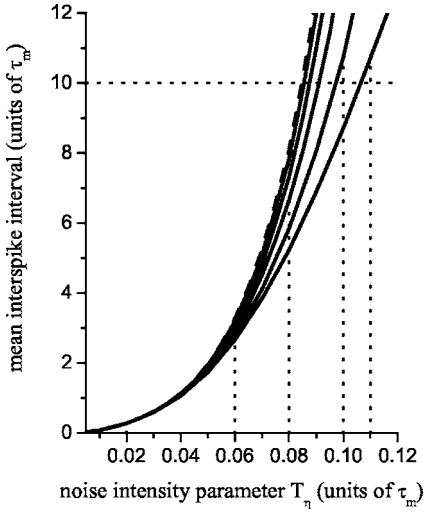

FIG. 6. Dependence of mean interspike interval on noise intensity parameter T_η. $w_\eta=0.5\hat{w}_s$, $T_s=10\tau_m$, w_s takes 0.0, 0.1, 0.3, 0.5, 0.7, and 0.9 $\hat{w}_s$ from the right-hand side to the left-hand side, respectively. The vertical dotted lines denote the optimal noise intensity parameter, and the level dotted line denotes the coherent input period.

gain at the optimal noise intensity becomes larger as the driving coherent signal becomes slower. Therefore, we can infer that the slower coherent signal in noisy environment is more possible to be detected by the integrate-and-fire (IF) neuron model (1).

Why is there only a SNR gain larger than unity in the weakest coherent coupling case? We turn to Eq. (1). Similar to the derivation of Eq. (3), the solution of Eq. (1) with $w_\eta \neq 0$ is given as

$$V(t) = \frac{w_s}{\tau_m}\sum_{n=0}^{n_1}\exp\left(-\frac{1}{\tau_m}(t-nT_s)\right)H(t-nT_s) + \frac{w_\eta}{\tau_m}\sum_{k=0}^{k_1}\exp\left(-\frac{1}{\tau_m}(t-t_k)\right)H(t-t_k), \qquad (11)$$

with $n_1=\max\{n:\ nT_s\leqslant t\}$, $k_1=\max\{k:\ t_k\leqslant t\}$. Noting that the first term is the dedication of the coherent component, and the second one is that of the random background activities, from Eq. (11) we know that for given T_s, τ_m, and w_η, if w_s is larger, $V(t)$ reaches the threshold easier. Thus in the case of larger coherent couplings, although the role of the synaptic noise is necessary, the event of $V(t)$ reaching the threshold is dominated by the coherent signal; while in the case of quite weak coherent couplings such as $w_s=0.1\hat{w}_s \ll w_\eta=0.5\hat{w}_s$ as shown in Fig. 2, whether $V(t)$ reaches the threshold is nearly completely dominated by the synaptic noise, namely, it is mainly the noise energy that converts into the power component of the output at the signal frequency $1/T_s$. This viewpoint is further confirmed in Fig. 6. Seen from the figure, for larger coherent couplings, the optimal noise intensity parameter is nearly the noise intensity parameter where the mean ISI is approximately equal to the coherent period such as in the cases of $w_s=0.7\hat{w}_s$ and $w_s=0.9\hat{w}_s$. But for weaker coher-

ent couplings, the approximate relation is not true anymore. Especially for the case of $w_s=0.1\hat{w}_s$, where the optimal noise intensity parameter $T_\eta^{\mathrm{opt}}\approx 0.02\tau_m$, there is no obvious matching relation between T_s and the mean ISI at T_η^{opt}. These analyses show that the physical mechanism behind the SR phenomenon in the weakest coherent coupling case and that behind the SR phenomenon in the larger coherent coupling case are different, and the former should be some kind of resonance induced by noise, which is responsible for the difference.

IV. CONCLUSIONS

We have extended the research of the SNR gain from peripheral sensory neurons that process analog stimuli to central neurons that operate with spikes. For noisy threshold input signals transmitted by an IF model, our investigation has disclosed that the SNR gain at the optimal noise intensity becomes larger as the coherent coupling increases for larger coherent couplings, but it cannot exceed unity. While for the weaker coherent couplings, the SNR gain at the optimal noise intensity becomes larger as the coherent coupling decreases, and among all the cases considered by us, there is a SNR gain larger than unity only for the weakest coherent coupling case owing to the noise-induced resonance. Thus, the shot noise might be more useful in assisting neurons to process the weakest periodic pulse trains. The investigation also suggests that for slow periodic spike trains, there is more possibility for a SNR gain larger than 1, which might be important in explaining that the brain sometimes is more sensitive to slower discrete subthreshold signals. The conclusions are expected to be useful in reflecting some common properties of real neurons that transmit subthreshold pulse modulations by means of shot noises. In future work, we will consider how the duration time of periodic pulses influences the SNR gain.

ACKNOWLEDGMENT

The work is partially supported by the National Natural Science Foundation of China (Grant No. 10432010).

[1] R. Benzi, A. Sutera, and A. Vupiani, J. Phys. A **14**, L453 (1981).
[2] L. Gammaitoni, P. Hanggi, P. Jung, and F Marchesoni, Rev. Mod. Phys. **70**, 223 (1998).
[3] N. G. Stocks, N. D. Stein, and P. V. E. McClintock, J. Phys. A **26**, L385 (1993).
[4] Y. M. Kang, J. X. Xu, and Y. Xie, Phys. Rev. E **68**, 036123 (2003).
[5] K. Wiesenfeld, D. Pierson, E. Pantazelou, C. Dames, and F. Moss, Phys. Rev. Lett. **72**, 2125 (1994).
[6] A. S. Pikovsky and J. Kurths, Phys. Rev. Lett. **78**, 775 (1997).
[7] L. B. Kiss, in *Chaotic, Fractal, and Nonlinear Signal Processing*, edited by R. Katz (American Institute of Physics, New York, 1996), p. 382.
[8] F. Chapeau-Blondeau, Phys. Lett. A **232**, 41 (1997).
[9] M. I. Dykman, D. G. Luchinsky, R. Mannella, P. V. E. McClintock, N. D. Stein, and N. G. Stocks II, Nuovo Cimento D **17D**, 661 (1995).
[10] K. Loerincz, Z. Gingl, and L. B. Kiss, Phys. Lett. A **224**, 63 (1996).
[11] Z. Gingl, R. Vajtai, and L. B. Kiss, Chaos, Solitons Fractals **11**, 1929 (2002).
[12] P. Makra, Z. Gingl, and T. Fulei, Phys. Lett. A **317**, 228 (2003).
[13] Z. Gingl, P. Makra, and R. Vajtai, Fluct. Noise Lett. **1**, L181 (2001).
[14] F. Liu, Y. Yu, and W. Wang, Phys. Rev. E **63**, 051912 (2001).
[15] J. Casado-Pascual, C. Denk, J. Gómez-Ordóñez, M. Morillo, and P. Hänggi, Phys. Rev. E **67**, 036109 (2003).
[16] M. Shidara, K Kawano, H. Gomi, and M. Kawato, Nature (London) **50**, 365 (1993).
[17] W. R. Softky and C. Koch, J. Neurosci. **13**, 334 (1993).
[18] F. Chapeau-Blondeau, X. Godivier, and N. Chambet, Phys. Rev. E **53**, 1273 (1996).
[19] L. Zhangcai and Q. Youguo, Phys. Rev. Lett. **91**, 208103 (2003).
[20] A. N. Burkitt and G. M. Clark, Neural Comput. **13**, 2639 (2001).
[21] K. I. Amemori and S. Ishii, Neural Comput. **13**, 2763 (2001).
[22] T. Shimokawa, K. Pakdaman, T. Ttakahata, S. Tanabe, and S. Sato, Biol. Cybern. **84**, 327 (2000).